Anisotropy of the electrical transport properties in a Ni₂MnGa single crystal: Experiment and theory

Min Zeng,[1] Meng-Qiu Cai,[2] Siu Wing Or,[3,a)] and Helen Lai Wa Chan[1,a)]

[1]*Department of Applied Physics, The Hong Kong Polytechnic University, Hung Hom, Kowloon, Hong Kong*
[2]*State Key Laboratory of Optoelectronic Materials and TechnologiesZhongshan University, Guangzhou 510275, Guangdong, People's Republic of China*
[3]*Department of Electrical Engineering, The Hong Kong Polytechnic University, Hung Hom, Kowloon, Hong Kong*

Electrical transport properties in ferromagnetic shape memory Ni–Mn–Ga single crystal have been investigated both in experiment and theory by analyzing electrical resistivity along different crystallographic directions during heating. The experimental results show a clear first-order martensitic transformation and a large anisotropic resistivity (AR) of 23.7% at the tetragonal martensitic phase. The theoretical conductivity ($\sigma = 1/\rho$), estimated using first-principles calculations combined with classical Boltzman transport theory, proves essential crystallographic anisotropic resistivity (AR=31%) in the martensitic phase and agrees well with experimental results. The AR in the martensitic phase is reveled to mainly originate from the splitting of the minority-spin Ni $3d$ and Ga $4p$ states near the Fermi level and hence reconstruction of the minority-spin Fermi surface upon martensitic transformation. © *2010 American Institute of Physics*. [doi:10.1063/1.3354105]

I. INTRODUCTION

Ferromagnetic shape memory alloy Ni–Mn–Ga, having giant magnetic field-induced strain (MFIS) up to 10%,[1] is a class of active materials for the potential application as actuator/transducer as well as sensor from a technological point of view.[2,3] The mechanism of giant MFIS originates from twin-variant movement in the martensitic phase under an external field as the result of high magnetic anisotropic energy (MAE).[4,5] Martensitic transformation makes key contribution to the forming of the twin variant. In the high temperature austenitic phase, the structure has been found to be in cubic L₁ ordering.[6] Upon cooling, there are three crystallographic equivalent directions for deformation and these martensites have either tetragonal or orthorhombic structure depending on the composition.[7] the twin-variant configuration, which associates with the minimization of energy, is formed with well-defined boundaries during the martensitic transformation.[8] Also, the twin-variant redistribution is clearly visualized by using high speed photography.[9] It is thus expect that when twin-variant motion occurs, various related properties of the crystal could change.

It is also the twin-variant redistribution that leads to the change in electrical resistance under the application of a magnetic field. Srivastava and Chatterjee[10] reported the effect of twin-variant movement on electrical resistivity (ρ) in a Ni–Mn–Ga single crystal and ascribed its mechanism to crystallographic anisotropic resistivity (AR). That is to say, the variation in electrical resistivity, which originates from the redistribution of the twin variant with different electrical resistivity, is controlled by a magnetic field. This magneti-cally controlled resistivity/resistance [referenced as magne-toresistance (MR) effect] shows a potential application in novel magnetic memory storage device.[11] Current study on the MR effect of Ni–Mn–Ga alloy have been mostly carried out in polycrystalline system,[12–14] where MR effect can be understood by spin transport mechanism that considered different magnetization processes in large ferromagnetic clusters and spin reorientation of small clusters and boundary spins. However, the study on the electrical resistivity in different single-variant state is rarely reported in experimental observation and theoretical calculation. Therefore, in order to address the issue, systematic experiment and theoretical calculation have been performed to study the resistivity for single-variant state of a Ni–Mn–Ga crystal. This is not only essential for the technological application in magnetic data storage by adjusting twin-variant configuration but also fundamental to insight into the MR physical mechanism in the Ni–Mn–Ga single crystal.

II. DETAILS OF EXPERIMENTAL AND THEORETICAL CALCULATION

The Ni-Mn-Ga single crystal, with a chemical composition $Ni_{49.2}Mn_{29.6}Ga_{21.2}$, dimensions 10(length)×5(width) ×1.1(thickness) mm³, the two major surfaces parallel to the {110} planes, and a dc-MFIS of 5.6% at room temperature, was provided by AdaptaMat Ltd. in Finland. The transformation temperatures were determined to be austenite start (A_s)=38 °C, austenite finish (A_f)=41 °C, martensite start (M_s)=35 °C, and martensite finish (M_f)=33 °C using a differential scanning calorimeter (Perkin Elmer DSC7). The crystal structure was characterized to be a five-layer martensite (5M) by using an x-ray diffractometer (Bruker AXS D8 Advance), the parameters in the unit cell are $a=b=5.94$ Å,

---
a)Authors to whom correspondence should be addressed. Electronic addresses: apahlcha@inet.polyu.edu.hk and eeswor@polyu.edu.hk.
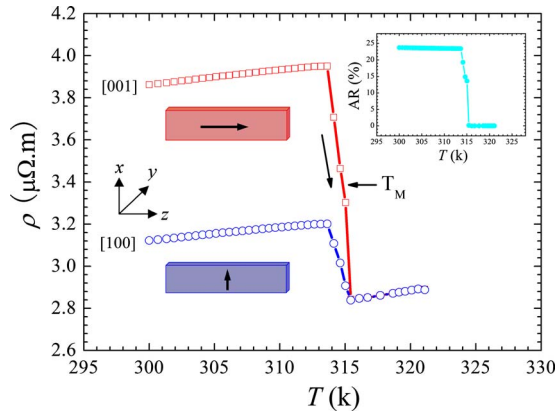
107, 083713-1

FIG. 1. (Color online) Electrical resistivity (ρ) dependence on temperature along the [001] and [100] directions of the Ni–Mn–Ga crystal during heating as well as single-variant configuration. The inset shows the AR dependence of temperature.

$c = 5.59$ Å for the martensitic phase, and $a = b = c = 5.82$ Å for the austenitic phase. The easy (c) and hard (a and b) axes of magnetization were along the [001] and [100]/[010] directions, respectively, as evaluated from the magnetization-field ($M-H$) curves using a vibrating sample magnetometer (Lakeshore 7600). Compared with the theoretical maximum lattice strain ($\varepsilon_0 = 1 - c/a$) of 5.89%, the two end points of 0% and 5.6% strains at room temperature were reasonable assumed to be the single-variant state. See the variant configurations in Fig. 1, the red block with an arrow "→" (easy axis orientation) and the blue block with an arrow "↑" denote the single-variant states with c and a axis parallel to sample length direction, respectively. The electrical resistivity (ρ) versus temperature (T) measurements were performed in the range of 300 K $\leq T \leq$ 321 K during heating. The usual 4-probe method was made with current flowing in the length direction of the crystal. Thus, we refer resistivity at the two strain end points of 0% and 5.6% in this paper as $\rho[001]$ and $\rho[100]$, respectively. (Here, $\rho[010]$ is omitted due to axes $a = b$.)

The electronic structure calculation was performed using the WIEN2K package.[15,16] In the course of calculation, we used simplified nonmodulated tetragonal structure with experimental lattice constants. The generalized gradient approximation potential within the Perdew, Burke, and Ernzerhof is used for the exchange correlation potential. And spin-orbit coupling along the [001] direction (easy axis) is included in the tetragonal structure, regarding as an origin for giving rise to a MAE.[17] The muffin-tin sphere radii are 2.25, 2.30, and 2.35 astronomical unit for Ni, Mn, and Ga, respectively. The plane wave cut-off for the scalar relativistic basic function are $R_{mt}K_{max} = 9$ and $l_{max} = 10$. Integrations in the reciprocal space for self-consistent field cycles were performed by using the tetrahedron method and an 75 k-points was used for both the cubic and tetragonal phases in the irreducible wedge of the Brillouin zone (BZ).

The theoretical conductivity coefficient (σ/τ, where τ is the relaxation time) was calculated by means of the classical Boltzmann transport theory.[18,19] The conductivity $\sigma_{\alpha\beta}$ is a product of transport tensors as functions of the temperature T and the chemical potential μ, expressed as

$$\sigma_{\alpha\beta}(T;\mu) = \frac{1}{\Omega}\int \sigma_{\alpha\beta}(\varepsilon)\left[-\frac{\partial f_u(T;\varepsilon)}{\partial \varepsilon}\right]d\varepsilon, \quad (1)$$

where $f_\mu(T;\varepsilon)$ is the Fermi–Dirac distribution. Since $-\partial f/\partial \varepsilon$ is a narrow bell-like function peaked at E_F with the width of the order k_bT, this restricts the relevant energy levels entering Eq. (1) to those in the close vicinity of the Fermi surface. The distribution $\sigma_{\alpha\beta}(\varepsilon)$ is the sum over the k points $\vec{k}$ and bands i

$$\sigma_{\alpha\beta}(\varepsilon) = \frac{1}{\Omega}\sum_{i,k} \tau(i,k)\nu_\alpha(i,k)\nu_\beta(i,k)\delta[\varepsilon(i,k) - E_F], \quad (2)$$

where $\varepsilon(i,k)$ is the band energy, $\nu_\alpha(i,k)$ the projection of band velocity ($\partial\varepsilon(i,k)/\partial k_\alpha$) on the α direction, $\tau(i,k)$ the relaxation time, and E_F is the Fermi energy. The calculation was performed by using the BOLTZTRAP program.[20] In the course of calculation, relaxation time is approximated as a constant, we can then obtain a quantitative conductivity tensor with respect to the accurate electronic eigenvalues calculated on a nonshifted mesh with 56 000 k points [3800 in the irreducible wedge of the Brillouin zone (IBZ)], which is four time as dense as the original. Thus, the resistivity can be evaluated from the conductivity, $\sigma = 1/\rho$. Note that the chemical potential μ equals to band energy obtained from first principle calculation.

III. RESULTS AND DISCUSSION

Figure 1 shows the electrical resistivity (ρ) as a function of temperature (T) of the Ni–Mn–Ga single crystal measured along the [001] and [100] directions during heating. The first-order martensitic transition at $T_M = 316.2$ K is clear. The significant resistivity difference is observed in the martensitic phase, while it is no absent in the austenitic phase. It is reasonable concluded that the crystallographic anisotropy of the resistivity in the tetragonal Ni–Mn–Ga crystal is appreciable: $\rho_{[001]} > \rho_{[100]}$. Dependence of temperature on the AR, defined as AR $= \rho[001] - \rho[100]/\rho[100]$, is shown in the inset in Fig. 1 which reveals that AR is found to be around 23.7% in the whole martensitic phase. Based on magnetically controlled twin-variants configuration,[4,5] the resistivity in martensitic phase is also magnetically controllable as pointed out in Ref. 6, which indicates an potential application in a new memory device.

The calculated conductivity properties as a function of chemical energy is shown in Fig. 2(a) for tetragonal Ni–Mn–Ga crystal at 300 K (conductivities are isotropic in the austenitic phase, not shown here). The anisotropic conductivity is well illustrated near the Fermi level and agrees well with the experimental results. At a quantitative level, the calculation yields $\sigma/\tau = 6.31 \times 10^{20}$ (Ω ms)$^{-1}$ in the [100] direction and 4.82×10^{20} (Ω ms)$^{-1}$ in the [001] direction. By using the constant relaxation time assumption, the calculation thus reproduced reasonable well the anisotropic nature of the resistivity at a quantitative level (AR = 31%). Furthermore, the temperature dependent conductivity near the Fermi energy is presented in Fig. 2(b) for both directions. It can be seen that the anisotropic behavior in the conductivity is re-
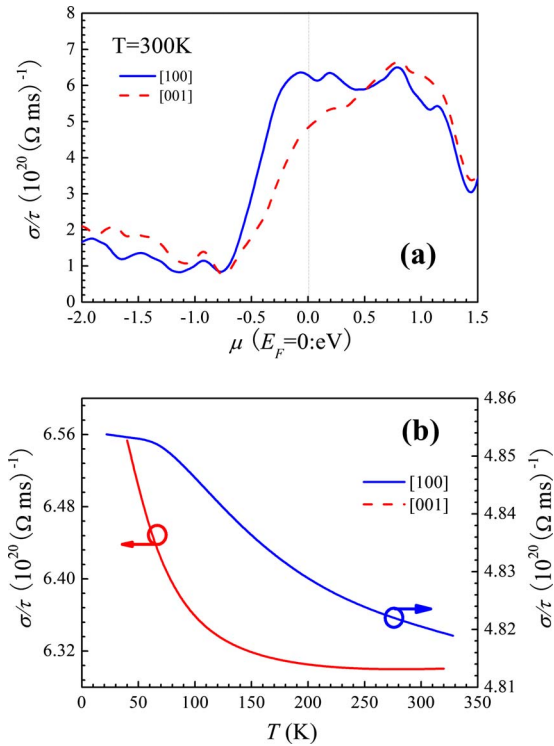
FIG. 2. (Color online) Theoretical anisotropic conductivity coefficient as a function of (a) chemical potential at 300 K and (b) temperature near Fermi level for the [100] and [001] directions of Ni–Mn–Ga crystal.

mained in whole low temperature range of martensitic phase, which proves the essential crystallographic anisotropy of the resistivity as shown in Fig. 1.

In order to investigate the physical mechanism and microscopic origin of the AR behavior, the electronic structure of Ni–Mn–Ga crystal is analyzed by the first principle calcu-lation with density function theory. The calculated total and partial density of states (PDOS) near the Fermi energy (E_F) are shown in Fig. 3 for the Ni–Mn–Ga crystal in the equilibrium martensitic and austenitic phases. It can be seen that, in the majority-spin states, there is no obvious difference between both phases, while, a significant difference between the two phases is observed in the minority-spin states. In the austenitic phase, the minority-spin DOS has a sharp peak around −0.19 eV. The peak is mainly dominated by Ni $3d$ state with a weak hybridization with Ga $4p$ state. Due to the tetragonal distortion in the martensitic phase, the Ni minority-spin $3d$ states splits into two peaks, one strong peak is shifted toward a lower energy and located at −0.371 eV. Another weak peak is excited above E_F and centered at 0.088 eV. The splitting is contributed to the band Jahn-Teller effect which stabilizes the martensitic phase.[21] Similar splitting is also observed in Ga $4p$ state. In contrast, Mn $3d$ state has no contribution to the band Jahn–Teller effect. It must be noted that the calculation of electronic structure as well as resistivity is performed in nonmodulated tetragonal structure. Zayak *et al.*[22] reported the electronic structure difference between nonmodulated and modulated tetragonal structure and described the opening of a pseudogap close to E_F as the result of the modulated tetragonal structure. In fact, the pseudogap opening is similar to the splitting near E_F in our calculation, indicating that our DOS can qualitatively reflects the electronic structure in the modulated tetragonal structure as those reported obtained previously.[23–25]

Since conductivity calculation heavily relies on the contribution of band of band across the E_F, it is more straightforward to demonstrate the properties of the conduction electrons by depicting the Fermi surfaces. Figure 4 displays the calculated majority-spin and minority-spin Fermi surfaces as
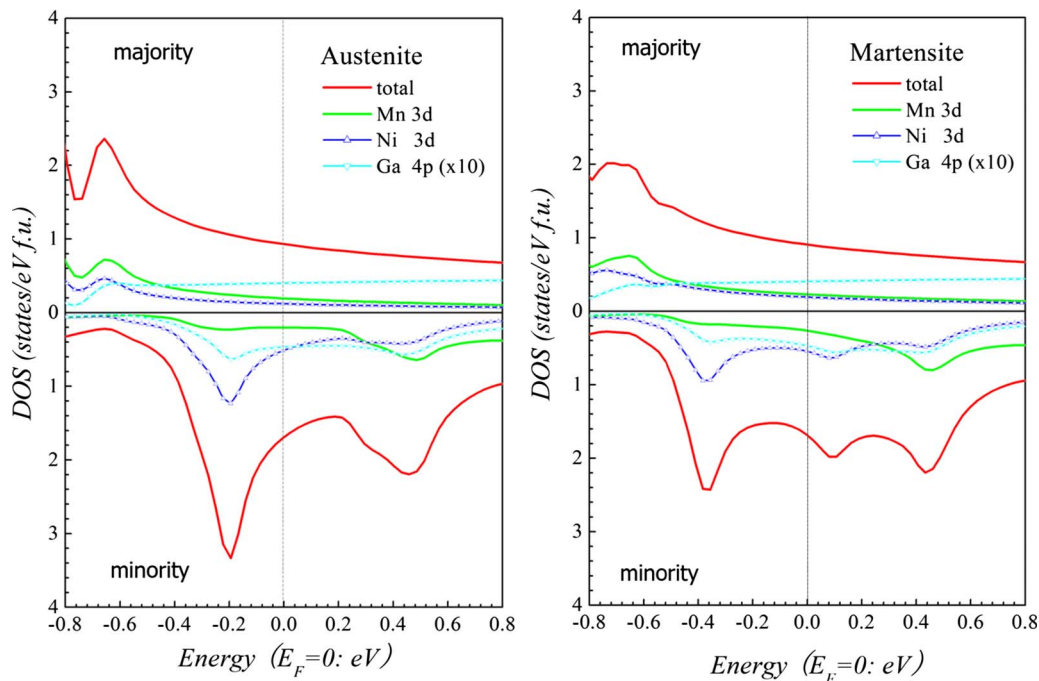

FIG. 3. (Color online) Majority- and minority-spin total DOS and PDOS of Ni-Mn-Ga crystal in the near E_F region in equilibrium (a) austenitic and (b) martensitic phases. The Ga p PDOS is multiplied by a factor of 10.
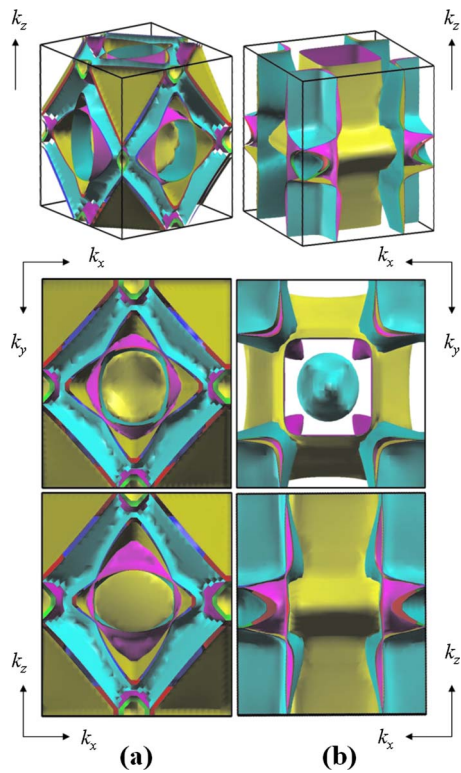
FIG. 4. (Color online) Fermi surfaces as well as the projection onto the k_x −k_y and k_x−k_z planes for (a) majority spin and (b) minority spin in the unit cell of tetragonal martensitic phase.

well as the projection of Fermi surfaces onto the k_x−k_y and k_x−k_z planes in the first BZ for the tetragonal martensitic phases by using the drawing program XCRYSDEN.[26] These Fermi surfaces are contributed by nine bands that cross E_F, resulting in a significant complexity of structure. Similar to the results reported by Opeil *et al.*,[27] the highly symmetric Fermi surfaces are presented in the austenitic phase as well as majority-spin state in the martensitic phase, while a large Fermi surface reconstruction only occurs in the minority-spin band martensitic phase. These differences in Fermi surfaces are similar to these in the DOS shown in Fig. 3, which confirms that the Fermi surface calculation is reliable. According to Eq. (1), the conductivity is proportional to the band velocity $\partial\varepsilon(i,k)/\partial k_\alpha$ that is normal to the Fermi surface,[28] we can further identified the mechanism of the large AR from the Fermi surfaces. From Fig. 4, it can be observed that the martensitic transformation results in only very tiny modification on the k_x−k_z projection plane of the majority-spin bands. This means that the band velocity is nearly isotropic, corresponding to an isotropic conductivity. However, the minority-spin Fermi surfaces are remarkably deformed. Except for the Fermi surfaces in the center of unit cell remain nearly intact, see the k_x−k_y projection plane, all other Fermi surfaces are reconstructed and formed a similar cylindrical shape along the k_z direction, see the k_x−k_z projection plane. That is to say, the band velocity produces an increasing component in the k_x−k_y plane, in which the Fermi surface is highly symmetrical, and a diminishing component in the k_z direction. It is thus concluded that the reconstruction of the minority-spin Fermi surfaces lead to the large crystallo-

graphic anisotropic conductivity: $\sigma_{[001]} < \sigma_{[100]}$. Consequently, the AR: $\rho_{[001]} > \rho_{[100]}$, which is consistent with the experimental result.

IV. CONCLUSIONS

In summary, we have presented the experimental and theoretical study of the electrical resistivity in Ni–Mn–Ga single crystal upon martensitic transformation. A crystallographic AR of 23.7% has been observed for the tetragonal martensitic phase in the experiment. The theoretical AR of 31%, calculated by using the first principle calculations combined with classical Boltzman transport theory, as emphasized, is in well agreement with experiment. The mechanisms that may cause a large AR have been recognized from our calculation. The electronic structure calculation reveals that the martensitic transformation results in the splitting of the minority-spin state near the Fermi level and the deformation of the minority-spin Fermi surface band leads to a highly anisotropic topology which is the origin of the anisotropy of resistivity in the tetragonal phase. It is reasonably concluded that Ni–Mn–Ga single crystal has a potential application in magnetic data storage by adjusting twin-variant configuration.

[1] A. Sozinov, A. A. Likhachev, N. Lanska, and K. Ullako, Appl. Phys. Lett. **80**, 1746 (2002).
[2] J. Tellinen, I. Suorsa, A. Jaaskelainen, I. Aaltio, and K. Ullakko, 8th International Conference ACTUATOR 2002, Bremen, Germany, 10–12 June 2002.
[3] N. Sarawate and M. Dapino, Appl. Phys. Lett. **88**, 121923 (2006).
[4] K. Ullakko, J. K. Huang, C. Kantner, R. C. O'Handley, and V. V. Kokorin, Appl. Phys. Lett. **69**, 1966 (1996).
[5] H. D. Chopra, C. Ji, and V. V. Kokorin, Phys. Rev. B **61**, R14913 (2000).
[6] P. J. Webster, K. R. A. Ziebeck, S. L. Town, and M. S. Peak, Philos. Mag. B **49**, 295 (1984).
[7] A. Sozinov, A. A. Likhachev, and K. Ullakko, IEEE Trans. Magn. **38**, 2814 (2002).
[8] S. J. Murray, M. A. Marioni, A. M. Kukla, J. Robinson, R. C. O'Handley, and S. M. Allen, J. Appl. Phys. **87**, 5774 (2000).
[9] S. J. Murray, M. Marioni, S. M. Allen, and R. C. O'Handley, Appl. Phys. Lett. **77**, 886 (2000).
[10] V. K. Srivastava and R. Chatterjee, J. Phys. D **40**, 4998 (2007).
[11] I. Stolichnov, S. W. E. Riester, H. J. Trodahl, N. Setter, A. W. Rushforth, K. W. Edmonds, R. P. Campion, C. T. Foxon, B. L. Gallagher, and T. Jungwirth, Nature Mater. **7**, 464 (2008).
[12] C. Biswas, R. Rawat, and S. R. Barman, Appl. Phys. Lett. **86**, 202508 (2005).
[13] V. O. Golub, A. Ya. Vovk, L. Malkinski, C. J. O'Connor, Z. Wang, and J. Tang, J. Appl. Phys. **96**, 3865 (2004).
[14] J. Marcos, A. Planes, L. Manosa, A. Labarta, and B. J. Hattink, Phys. Rev. B **66**, 054428 (2002).
[15] P. Blaha, K. Schwarz, G. K. H. Madsen, D. Kvasnicka, and J. Luitz, *WIEN2K*, (Technical University of Vienna, Austria, 2001).
[16] M. Q. Cai, Y. J. Zhang, Z. Yin, and M. S. Zhang, Phys. Rev. B **72**, 075406 (2005).

[17]J. Enkovaara, A. Ayuela, L. Nordstrom, and R. M. Nieminen, Phys. Rev. B **65**, 134422 (2002).

[18]R. Gómez Abal, A. M. Llois, and M. Weissmann, Phys. Rev. B **53**, R8844 (1996).

[19]T. J. Scheidemantel, C. Ambrosch-Draxl, T. Thonhauser, J. V. Badding, and J. O. Sofo, Phys. Rev. B **68**, 125210 (2003).

[20]G. K. H. Madsen and D. J. Singh, Comput. Phys. Commun. **175**, 67 (2006).

[21]S. Fujii, S. Ishida, and S. Asano, J. Phys. Soc. Jpn. **58**, 3657 (1989).

[22]A. T. Zayak, P. Entel, J. Enkovaara, A. Ayuela, and R. M. Nieminen, J. Phys.: Condens. Matter **15**, 159 (2003).

[23]V. V. Godlevsky and K. M. Rabe, Phys. Rev. B **63**, 134407 (2001).

[24]S. R. Barman, S. Banik, and A. Chakrabarti, Phys. Rev. B **72** 184410 (2005).

[25]C. Bungaro, K. M. Rabe, and A. D. Corso, Phys. Rev. B **68**, 134104 (2003).

[26]Z. Y. Zhu, H. W. Zhang, S. F. Xu, J. L. Chen, Z. X. Cao, and G. H. Wu, J. Appl. Phys. **103**, 093704 (2008) (Code available from http://www.xcrysden.org).

[27]C. P. Opeil, B. Mihaila, R. K. Schulze, L. Mañosa, A. Planes, W. L. Hults, R. A. Fisher, P. S. Riseborough, P. B. Littlewood, J. L. Smith, and J. C. Lashley, Phys. Rev. Lett. **100**, 165703 (2008).

[28]V. N. Antonov, A. Ya. Perlov, P. M. Oppeneer, A. N. Yaresko, and S. V. Halilov, Phys. Rev. Lett. **77**, 5253 (1996).